



Contents lists available at ScienceDirect

Bioorganic & Medicinal Chemistry Letters

journal homepage: www.elsevier.com/locate/bmcl

Synthesis, biological evaluation, hydration site thermodynamics, and chemical reactivity analysis of α -keto substituted peptidomimetics for the inhibition of *Plasmodium falciparum*



David J. Weldon^{a,e}, Falgun Shah^a, Amar G. Chittiboyina^{a,d}, Anjaneyulu Sheri^a, Raji Reddy Chada^a, Jiri Gut^b, Philip J. Rosenthal^b, Develeena Shivakumar^c, Woody Sherman^c, Prashant Desai^a, Jae-Chul Jung^a, Mitchell A. Avery^{a,d,*}

^aSchool of Pharmacy, Department of Medicinal Chemistry, University of Mississippi, University, MS 38677, United States

^bDepartment of Medicine, San Francisco General Hospital, University of California, San Francisco, CA 94143, United States

^cSchrodinger, Inc., 120 West 45th Street, 17th Floor, New York, NY 10036, United States

^dNational Center for Natural Products Research, University of Mississippi, University, MS 38677, United States

^eSchool of Pharmacy, Department of Pharmaceutical Sciences, Loma Linda University, Loma Linda, CA 92350, United States

ARTICLE INFO

Article history:

Received 6 January 2014

Accepted 21 January 2014

Available online 31 January 2014

Keywords:

Malaria
Peptidomimetic
Falcipain
Cruzain
Drug resistance

ABSTRACT

A new series of peptidomimetic pseudo-prolyl-homophenylalanylketones were designed, synthesized and evaluated for inhibition of the *Plasmodium falciparum* cysteine proteases falcipain-2 (FP-2) and falcipain-3 (FP-3). In addition, the parasite killing activity of these compounds in human blood-cultured *P. falciparum* was examined. Of twenty-two (22) compounds synthesized, one peptidomimetic comprising a homophenylalanine-based α -hydroxyketone linked Cbz-protected hydroxyproline (**39**) showed the most potency (IC₅₀ 80 nM against FP-2 and 60 nM against FP-3). In silico analysis of these peptidomimetic analogs offered important protein–ligand structural insights including the role, by WaterMap, of water molecules in the active sites of these protease isoforms. The pseudo-dipeptide **39** and related compounds may serve as a promising direction forward in the design of competitive inhibitors of falcipains for the effective treatment of malaria.

© 2014 Elsevier Ltd. All rights reserved.

Malaria, a parasitic disease caused by several plasmodial species, the most virulent of which in humans is *Plasmodium falciparum*, is a major health concern in Asia, South America, and sub-Saharan Africa. With an estimated 219 million cases resulting in 660,000 deaths worldwide in 2010,¹ the need for inexpensive, easy to use, and well-tolerated treatment options is clear. The first known treatment of malaria occurred in 1631 with the bark of the cinchona tree, from which quinine was later purified.² As quinine is not well tolerated, new therapeutics were developed, including chloroquine and related aminoquinolines, antifolates, and mefloquine. However, strains of *P. falciparum* resistant to all of the aforementioned therapeutics have been observed.^{3–5} Artemisinin, a natural product from *Artemisia annua*, and its derivatives have been identified as rapidly active and highly efficacious antimalarials.⁵ In recent years the standard of care for the treatment of uncomplicated *falciparum* malaria has moved to artemisinin-based combination therapy (ACT), which combines either artesunate, artemether, or dihydroartemisinin with a longer acting agent.⁶

* Corresponding author. Tel.: +1 662 915 5879; fax: +1 662 915 5638.

E-mail addresses: mavery@olemiss.edu, mitchellavery@att.net (M.A. Avery).

<http://dx.doi.org/10.1016/j.bmcl.2014.01.062>

0960-894X/© 2014 Elsevier Ltd. All rights reserved.

Recently, *P. falciparum* strains have shown decreased responsiveness to artemisinin therapy, leading to delayed parasite clearance after therapy, primarily near border areas of Thailand.³ This finding validates a continued search for effective alternative therapeutics targeting key pathways in the life cycle of malaria parasites. Among potential malarial drug targets, the cysteine proteases falcipain-2 (FP-2) and falcipain-3 (FP-3) were identified as mediators of the degradation of hemoglobin, which is required by erythrocytic malaria parasites to provide amino acids for parasite metabolism.^{7,8} Since the degradation of hemoglobin is essential for the survival of the parasite, the inhibition of FP-2 and FP-3 is a viable approach for the effective treatment of malaria.^{9–13} Several studies have validated FP-2/FP-3 as drug targets for chemotherapy of *P. falciparum* but both FP-2 and FP-3 must be inhibited simultaneously to achieve parasite death.^{14,15,11} Crystal structures of FP-2 (PDB codes 1YVB, 2GHU and 3BPF) were published in 2006^{16,17} and 2009.¹⁸ Fortunately, the crystal structure revealed the active sites of FP-2 and FP-3 to be quite similar, with some narrowing of the S₂ subsite in FP-3 compared to FP-2.^{19,20} Additionally, it was known that the falcipain proteases are closely related to cruzain proteases (**1** is the ligand from cruzain crystal

structure 1F29, PDB code) in structure in the active site.²⁰ This computational information, coupled with the report by Ellman and others²¹ of compound **2** as a peptidomimetic inhibitor of cruzain, we proceeded with docking studies of cruzain inhibitor **2** in FP-2. The studies revealed that inhibitors of cruzain would be a good starting structural motif for the design of novel inhibitors of falcipain cysteine proteases. The overlap in structural features of our designed motif **3** and the cruzain inhibitor **2** are shown in blue in Figure 1.

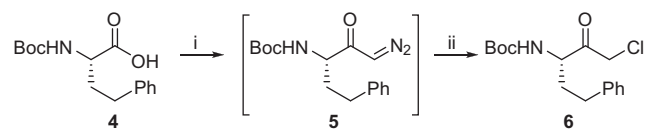
Of particular note, one of the phenylalanine residues in **2** has been replaced with a homophenylalanine in **3** and one of the carboxybenzyl-protected (Cbz-protected) phenylalanine amino acids in **2** has been replaced with a relatively constrained Cbz-protected proline derivative in **3**. The use of unnatural amino acids was deliberately made for two reasons: to by-pass peptidase metabolism, thereby increasing the compound half-life; and to decrease analog flexibility to improve binding thermodynamics. For the later, utilization of cyclic derivatives such as β -amino acids was appropriate. To probe the available 3D-chemical space for the substrate binding site of FP-2 and to explore the SAR, we designed and synthesized twenty-two compounds (**21–42**) from readily available building blocks.

The syntheses of the twenty-two pseudopeptidic cysteine protease inhibitors are dependent upon the construction of a homophenylalanine-based scaffold representing the C-terminus: an α -substituted ketone intended to interact with the catalytic cysteine thiol moiety; and the N-terminal residue. Peptide-like coupling of the α -chloroketone corresponding to homophenylalanine, **6**, with N-Cbz proline gives such a pseudodipeptide (**3**).

Specifically, synthesis of the α -chloroketone **6** was accomplished by in situ activation of the amino acid **4** as its mixed anhydride followed by quench with diazomethane to yield the diazoketone **5**, best immediately converted to the more stable α -chloroketone **6** with HCl in AcOH (Scheme 1). We chose eleven different synthetic amino acids for coupling to **6**, N-terminal residues which occupy the opposing S_2/S_3 site of falcipain. Hence, the Boc-group of **6** was removed with 2 M HCl in ether and the resulting amine-HCl salt **7** was then coupled with the eleven Cbz-protected unnatural amino acids furnishing the target compounds **9–20** (Scheme 2).

The N-terminal amino acids were all cyclic except for the use of a homophenylalanine (e.g. **36**). Most of these amino acids were β -amino acids, normally *cis*, and include β,β (e.g. **26**) or α,α (**27**) 1-aminocyclohexyl carboxylic acids. While the amino acids used for peptide coupling are denoted as R in Scheme 2 for the sake of simplicity, the exact structural details of the final compounds are shown in Figure 2. The reactive α -chloroketone of the derivatives was easily displaced by O, N, or S nucleophiles resulting in twenty-two target derivatives, **21–42** (Scheme 3).

The synthesized peptidomimetics were tested against FP-2 and FP-3 isoforms in vitro. Additionally, in vitro growth inhibition



Scheme 1. Synthesis of α -chloroketone **6**. Reagents and conditions: (i) 4-Methylmorpholine, isobutyl chloroformate, 1 h, reflux; THF, 0 °C, CH_2N_2 , 2 h, 72%; (ii) HCl-AcOH (1:1), ether, 0 °C, 1 h, 89%.

studies against the W2-strain (chloroquine resistant) of *P. falciparum* were also carried out.^{8,19,22–25} The biological activities of the derivatives are summarized in Table 1. While several peptidomimetics showed moderate activity in one of the three biological tests, compound **39** was clearly a superior candidate in both isoforms of FP-2, FP-3, and W2 inhibition of 80 nM, 60 nM, and 7.70 μM respectively.

In an attempt to understand the SAR of the peptidomimetics, we first considered the binding affinity in the active site of FP-2 and FP-3. From the experimental SAR, it was evident that hydroxyl proline in the S_2 pocket, an α -hydroxyketone electrophile in the S_1 - S_2' pocket, and homophenylalanine in the S_1 pocket were suitable substituents for high binding affinity peptidomimetics. Interestingly, efforts to understand the SAR of this series by means of steric and electrostatic interactions derived from the docking studies in FP-2 and FP-3 were not sufficient to explain the variation in biological data. Van der Waals energy, electrostatics, hydrogen bonds, or Docking Score from Glide SP^{26,27} docking calculations did not provide a statistical correlation with experimental binding affinity. Furthermore, implicit solvent binding energy estimations from MM-GBSA (as implemented in the program Prime)^{28,29} did not show a significant correlation with experimental binding affinity.

In light of the above findings, we anticipated the involvement of water molecules in the binding of these inhibitors, since explicit water solvation is neglected from all of the above analyses. Therefore, we generated thermodynamic profiles of water molecules present in the ligand binding domain (LBD) of FP-2 and FP-3 using WaterMap (Schrodinger, LLC) in an attempt to understand the observed SAR among the designed pseudopeptidomimetics. WaterMap computes the location and energetics of water molecules around a protein using explicit solvent molecular dynamics (MD), solvent clustering, and statistical thermodynamics.^{30,31} WaterMap was chosen to study the protein solvation effects because it has been effectively applied to a broad range of pharmaceutically relevant targets including PDZ domains,³² kinases,³³ G-protein coupled receptors (GPCRs),³⁴ protein-protein interaction interfaces,³⁵ and serine proteases.³⁶ Recently, a WaterMap study was reported by our group to understand binding modes of small molecule inhibitors of falcipain (FP-2 & FP-3) identified by virtual screening.³⁷

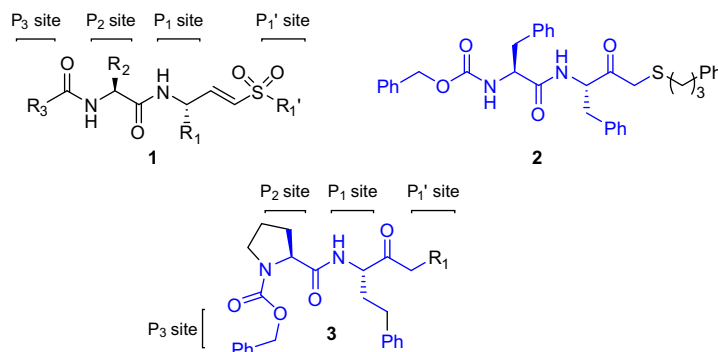
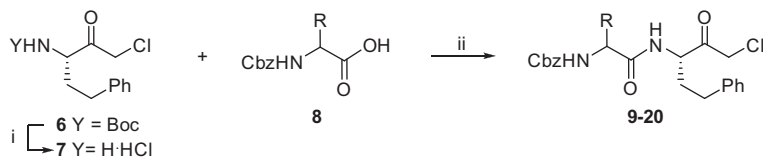


Figure 1. Structural similarity of vinyl sulfone ligand **1** from the cruzain crystal structure and cruzain inhibitor **2** with our designed inhibitor **3**.



Scheme 2. Synthesis of natural and unnatural dipeptide analogues. Reagents and conditions: (i) 2 M HCl in Et₂O, 0 °C to rt, 1 h; (ii) EDC, HOBT, triethylamine, DCM, 12 h.

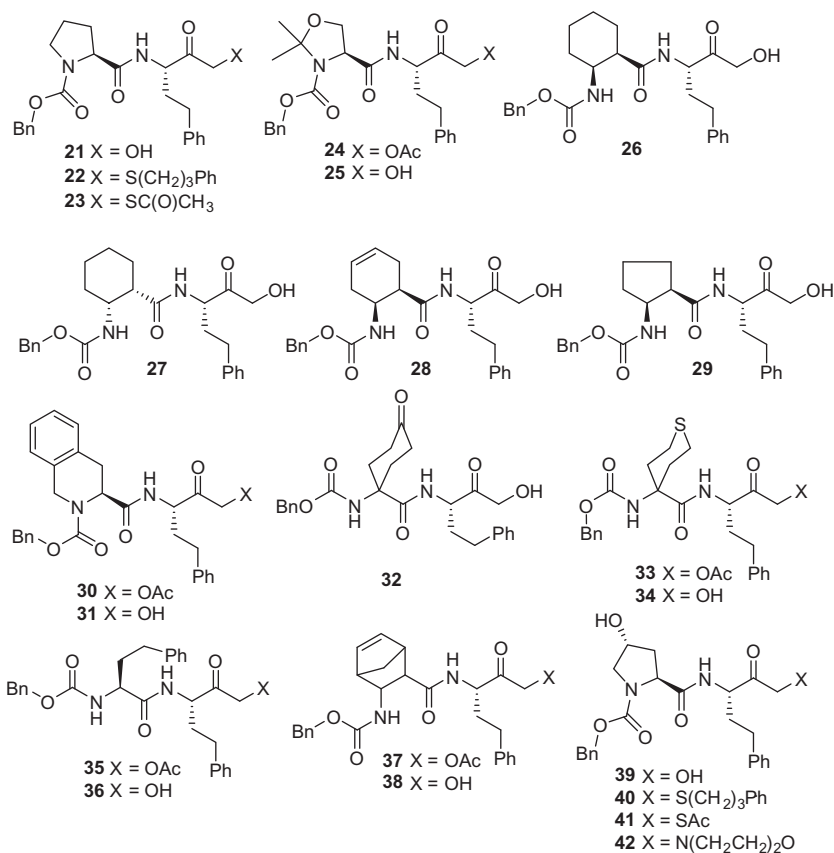
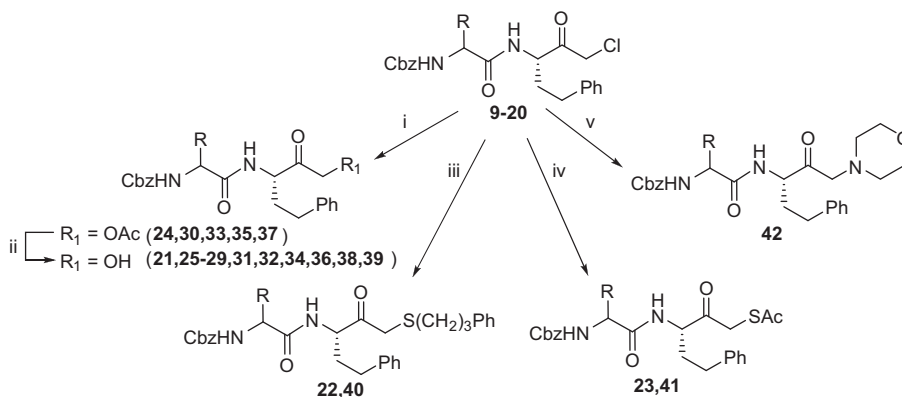


Figure 2. Peptidomimetic inhibitors explored in this work.



Scheme 3. Synthesis of target molecules. Reagents and conditions: (i) NaOAc, 18-crown-6, DMF, rt, 12 h, 91%; (ii) LiOH/H₂O, THF/H₂O, rt, 92%; (iii) 3-phenylpropane-1-thiol, triethylamine, THF, rt, 12 h, 83% (iv) KSac, DMF, rt, 12 h, 81%; (v) morpholine, triethylamine, THF, rt, 12 h, 84%.

WaterMap analysis was performed on the published crystal structures of FP-2 (3BPF, PDB code) and FP-3 (3BWK, PDB code) using default settings. The WaterMap calculations of the apo protein revealed several highly unstable water molecules in the LBD of FP-2

and FP-3, which could be displaced to yield improved binding energies.

Typically, water molecules with unfavorable (i.e. positive) free energy should be displaced by ligand functional groups to gain

Table 1
The biological activity of designed peptidomimetic analogues

Compds	Falcpain-2 Inhibition IC ₅₀ (μM)	Falcpain-3 Inhibition IC ₅₀ (μM)	Indochina clone W2 IC ₅₀ (μM)
21	>50	>50	>50
22	48.13	>50	13.77
23	>50	36.36	18.12
24	>50	>50	>50
25	>50	>50	>50
26	5.52	0.54	>50
27	4.42	0.91	47.60
28	>50	20.18	>50
29	>50	23.90	>50
30	>50	>50	>50
31	>50	>50	>50
32	>50	47.23	23.29
33	33.86	>50	>50
34	3.25	8.22	28.16
35	29.67	>50	>50
36	30.08	11.91	37.21
37	>50	>50	>50
38	33.64	25.44	47.21
39	0.08	0.06	7.70
40	1.10	0.52	19.64
41	>50	3.56	18.64
42	>50	>50	10.16

binding free energy through release of the water molecule into bulk solvent. Conversely, water molecules with negative free energy values should be bridged, judiciously replaced with the polar atoms of ligands to make the same interactions as the water,³⁸ or avoided altogether. Waters with negative ΔG also have negative enthalpy (ΔH), because the entropy contribution ($-T\Delta S$) is, by definition, always unfavorable for waters in the binding site relative to water molecules in bulk solution. Given the above considerations, the emerging SAR trends of peptidomimetics derivatives can be explained here in the context of the most active compound **39**. The WaterMap hydration sites in FP-2 and FP-3 binding sites along with compound **39** are shown in Figure 3.

According to the hydration site analysis, the homophenylalanine in the S₁ pocket displaces unfavorable water sites (W19 and W23 in FP-2; W14 and W19 in FP-3) in both enzymes. In addition, the proline hydroxyl group of **39** successfully displaces the most unstable hydration site in the S₁ binding pocket of both falcpains (W1, $\Delta G = 4.6$ kcal mol⁻¹ in FP-2; W1, $\Delta G = 4.3$ kcal mol⁻¹ in FP-3). The hydroxyl also forms an H-bond with the backbone of His174/

184, affording an additional boost in potency. Finally, the hydroxyproline moiety displaces two other unfavorable hydration sites (W5 and W12 in FP-2; W5 and W6 in FP-3 with $\Delta G \geq 2.3$ kcal mol⁻¹ from both enzymes). Compound **39** also displaces W10 in FP-2 ($\Delta G = 2.6$ kcal mol⁻¹) and W2 in FP-3 ($\Delta G = 4.2$ kcal mol⁻¹), with the replacement of a critical hydrogen bond with Gly83, which is considered important for binding to the non-prime site by inhibitors of papain family cysteine proteases.³⁹ A portion of the boost in potency of **39** can be attributed to its proline hydroxyl substituent displacing highly unstable water sites of the S₂ pocket, as the hydration site displacement pattern is the primary difference between **39** and the other derivatives.

The Cbz moiety of **39** also displaces several unfavorable water sites from the S₃ pocket of FP-2 and FP-3 (W4, W14, W16, and W20 in FP-2; W7, W8, W17, and W18 in FP-3) into the bulk of the solvent, and is a suitable substituent for the S3 pocket. The carbonyl moiety of the α -hydroxyketone in **39** displaces the proximal unstable water (W7 in FP-2, $\Delta G = 3.0$ kcal mol⁻¹, W16 in FP-3, $\Delta G = 1.4$ kcal mol⁻¹) from the S₁ pocket and replaces its H-bond interaction with the side chain of Gln36/45 and backbone of Cys42/52 in FP-2 and FP-3, respectively. The hydroxyl group of the α -hydroxyketone forms an H-bond with His 174/184 in FP-2 and FP-3. Additionally, the hydroxyketone stabilizes the unfavorable water molecule of the S₁' pocket (W22 in FP-2 with $\Delta G = 1.1$ kcal mol⁻¹; W4 in FP-3 with $\Delta G = 3.6$ kcal mol⁻¹) by forming a water-mediated H-bond with Trp (206/215) in both enzymes. To validate the WaterMap analysis, we evaluated derivatives with low and moderate activity to establish their ability to displace the unfavorable waters. The inactivity of **21**, a proline version of **39**, can be explained by the inability to displace the unfavorable water sites in the S₂ pocket (Fig. 4a). The moderate activity of **26** is a combination of the formation of a strong H-bond network with Gly83 in addition to the displacement of a few unfavorable water sites ($\Delta G \geq 2.3$ kcal mol⁻¹) of the S₂ pocket of FP-2 (Fig. 4b).

WaterMap was not able to provide insights about the preference of α -hydroxyketone in the S₁-S₁' pocket over other electrophiles with similar hydration site displacement characteristics. This might be expected, given that WaterMap only accounts for solvent displacement and not direct interactions made with the receptor. We anticipate that the reactivity of the carbonyl carbon in the vicinity of catalytic cysteine [42(FP-2)/52 (FP-3)] with different α -substituents might play an important role in the activity of these compounds.

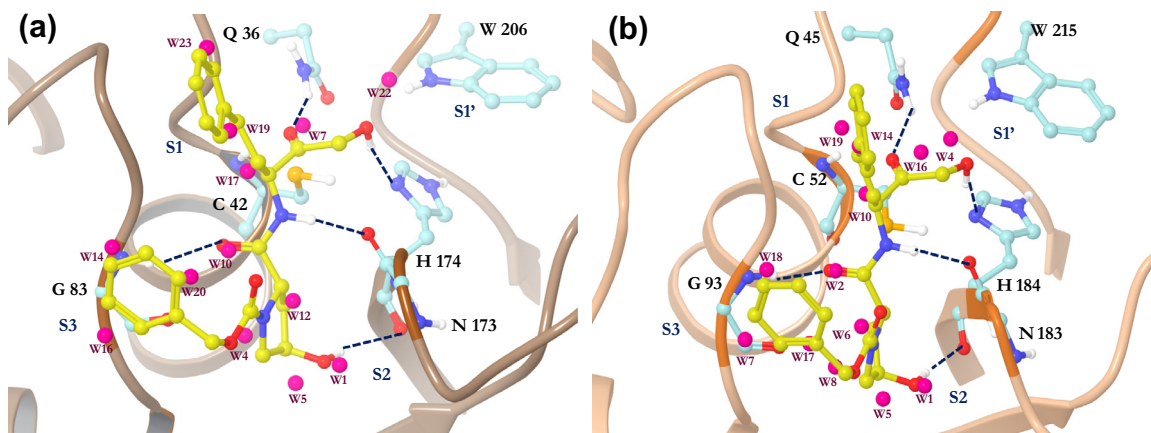


Figure 3. The WaterMap profile of **39** in (a) FP-2 and (b) FP-3 is shown. The thermodynamically interesting hydration sites important for SAR are shown in spheres. The unstable hydration sites ($\Delta G > 1$ kcal mol⁻¹) are shown in purple. The water sites are labeled based on decreasing value of predicted ΔG . Key hydrogen bonding interactions of **39** (shown in yellow) with the falcpain binding (shown in cyan) site residues are displayed.

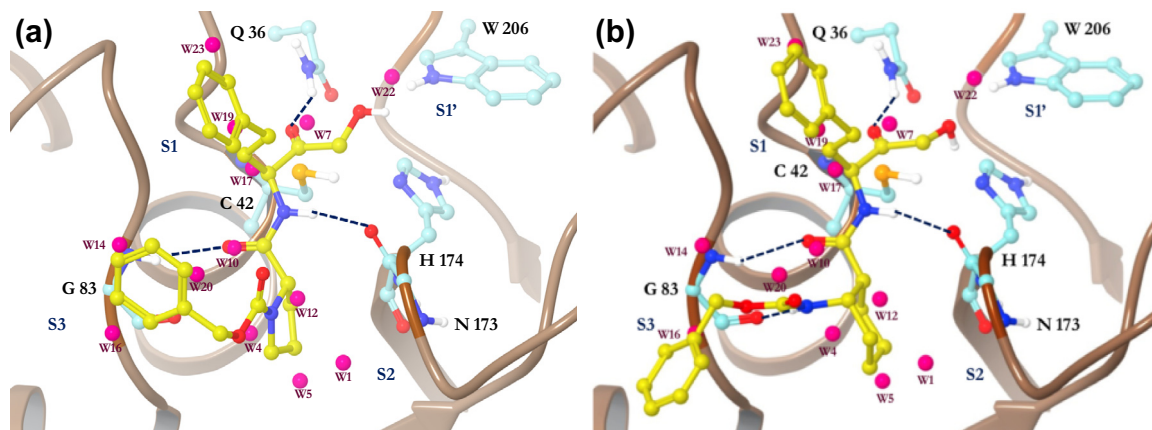


Figure 4. The predicted binding poses and interesting hydration sites for (a) **21** and (b) **26** are shown FP-2 isoform. Hydration sites labeling and color codes are same as shown in Figure 3.

Table 2
Predicted LUMO density of the most electrophilic center (shown by asterisk *) in compound **39–42**

Compds	Functional Group	F_NN_LUMO values
39		0.52
40		0.46
41		0.26
42		0.01

To help understand the reactivity of electrophiles with the catalytic cysteine residue and its effect on the inhibitory activity, we calculated the LUMO variant of Atomic Fukui indices at constant spin density using the quantum mechanics package Jaguar, as described previously.¹⁹ The compounds **39–42** with different electrophilic groups were considered for these calculations. The LUMO variant of Fukui indices was considered for predicting electrophilicity of the carbonyl carbon. The predicted LUMO values were scaled from zero to one, one being the most reactive, and are shown in Table 2. The predicted reactivity of electrophiles was higher for the compound with an α -hydroxyketone (**39**, LUMO = 0.52) than the compound with an α -thioketone (**40**, LUMO = 0.46; **41**, LUMO = 0.26), which in turn had a higher electrophilicity than the α -amino ketone (**42**, LUMO = 0.01). The calculated LUMO density values predict correct ordering of the inhibition of FP-2 and FP-3 for compounds **39–42**. These reactivity calculations complement the hydration site thermodynamic analysis and provide additional insights into the SAR of the compounds explored in this work.

In addition to elucidating the unfavorable waters that are displaced by **39**, WaterMap also predicts other unfavorable waters in the ligand-binding domain of FP-2 and FP-3 that were not

explored in this work. For example, WaterMap predicts unstable water (W3 in FP-2 with $\Delta G = 3.7$ kcal mol⁻¹; W9 in FP-3 with $\Delta G = 2.5$ kcal mol⁻¹) interacting with the backbone carbonyl of Ile85/87 lining the S₂ pocket of the proteases. W9 is also present in the X-ray structure of FP-3.⁴⁰ Moreover, WaterMap shows a network of stable waters (W24–W26 in FP-2 with $\Delta G = <-2.0$ kcal mol⁻¹; W21 and W22 in FP-3 with $\Delta G = <-0.7$ kcal mol⁻¹) at the bottom of the S₂ pocket forming an H-bond with Asp234 in FP-2 and Glu243 in FP-3. These water sites can be either targeted (functionally replacing the stable waters) or interacted with (water-mediated H-bonds) in future work to gain additional binding affinity.

The information gained from these computational analyses can be used to design the next generation of inhibitors of falcipains. Specifically, we plan to synthesize compounds that are able to displace unstable hydration sites that were not displaced by the compounds presented in this work. This may require developing new chemical scaffolds, as some of the unstable hydration sites are not accessible with the R-group positions in the chemotypes presented in the current manuscript. Further design efforts against FP-2 and FP-3 will consider the reactivity of electrophiles in addition to the displacement of unfavorable waters, in particular from the S₂ pocket of FP-2 and FP-3.

Acknowledgments

We thank the CDC cooperative agreements 1U01 CI000211-03 and 1U01 CI000362-01 for financial support. Additionally, Investigation was conducted in a facility constructed with support from Research Facilities Improvement Program Grant Number C06 RR14503-01 from the National Center for Research Resources, National Institutes of Health. We are grateful for WaterMap software support from Schrodinger, LLC.

References and notes

- World Malaria Report 2012; WHO Press, 2011. http://www.who.int/malaria/publications/world_malaria_report_2012/en (accessed on December 18th 2013).
- Toovey, S. The Miraculous Fever Tree. The Cure that Changed the World. Fiametta Rocco; Harper Collins: San Francisco, 2004, 348 pages, Paperback, ISBN 0-00-6532357.
- Dondorp, A. M.; Nosten, F.; Yi, P.; Das, D.; Phyo, A. P.; Tarning, J.; Lwin, K. M.; Arie, F.; Hanpithakpong, W.; Lee, S. J.; Ringwald, P.; Silamut, K.; Imwong, M.; Chotivanich, K.; Lim, P.; Herdman, T.; An, S. S.; Yeung, S.; Singhasivanon, P.; Day, N. P.; Lindgardh, N.; Socheat, D.; White, N. J. *N. Engl. J. Med.* **2009**, *361*, 455.
- Price, R. N.; Uhlemann, A. C.; Brockman, A.; McGready, R.; Ashley, E.; Phaipun, L.; Patel, R.; Laing, K.; Loareesuwan, S.; White, N. J.; Nosten, F.; Krishna, S. *Lancet* **2004**, *364*, 438.

5. Wellems, T. E.; Plowe, C. V. *J. Infect. Dis.* **2001**, *184*, 770.
6. Nosten, F.; White, N. J. *J. Trop. Med. Hyg.* **2007**, *77*, 181.
7. Sijwali, P. S.; Shenai, B. R.; Gut, J.; Singh, A.; Rosenthal, P. J. *Biochem. J.* **2001**, *360*, 481.
8. Sijwali, P. S.; Rosenthal, P. J. *Proc. Natl. Acad. Sci. U.S.A.* **2004**, *101*, 4384.
9. Rosenthal, P. J. *Int. J. Parasitol.* **2004**, *34*, 1489.
10. Rosenthal, P. J.; Sijwali, P. S.; Singh, A.; Shenai, B. R. *Curr. Pharm. Des.* **2002**, *8*, 1659.
11. Rosenthal, P. J.; Lee, G. K.; Smith, R. E. *J. Clin. Invest.* **1993**, *91*, 1052.
12. Rosenthal, P. J.; McKerrow, J. H.; Aikawa, M.; Nagasawa, H.; Leech, J. H. *J. Clin. Invest.* **1988**, *82*, 1560.
13. Rosenthal, P. J.; Olson, J. E.; Lee, G. K.; Palmer, J. T.; Klaus, J. L.; Rasnick, D. *Antimicrob. Agents Chemother.* **1996**, *40*, 1600.
14. Shenai, B. R.; Lee, B. J.; Alvarez-Hernandez, A.; Chong, P. Y.; Emal, C. D.; Neitz, R. J.; Roush, W. R.; Rosenthal, P. J. *Antimicrob. Agents Chemother.* **2003**, *47*, 154.
15. Rosenthal, P. J.; Wollish, W. S.; Palmer, J. T.; Rasnick, D. *J. Clin. Invest.* **1991**, *88*, 1467.
16. Wang, S. X.; Pandey, K. C.; Somoza, J. R.; Sijwali, P. S.; Kortemme, T.; Brinen, L. S.; Fletterick, R. J.; Rosenthal, P. J.; McKerrow, J. H. *Proc. Natl. Acad. Sci. U.S.A.* **2006**, *103*, 11503.
17. Hogg, T.; Nagarajan, K.; Herzberg, S.; Chen, L.; Shen, X.; Jiang, H.; Wecke, M.; Blohmke, C.; Hilgenfeld, R.; Schmidt, C. L. *J. Biol. Chem.* **2006**, *281*, 25425.
18. Kerr, I. D.; Lee, J. H.; Pandey, K. C.; Harrison, A.; Sajid, M.; Rosenthal, P. J.; Brinen, L. S. *J. Med. Chem.* **2009**, *52*, 852.
19. Shah, F.; Mukherjee, P.; Gut, J.; Legac, J.; Rosenthal, P. J.; Tekwani, B. L.; Avery, M. A. *J. Chem. Inf. Model.* **2011**, *51*, 852.
20. Sabnis, Y.; Rosenthal, P. J.; Desai, P.; Avery, M. J. *Biomol. Struct. Dyn.* **2002**, *5*, 765.
21. Huang, L.; Lee, A.; Ellman, J. A. *J. Med. Chem.* **2002**, *45*, 676.
22. Sabnis, Y. A.; Desai, P. V.; Rosenthal, P. J.; Avery, M. A. *Prot. Sci.* **2003**, *12*, 501.
23. Shah, F.; Mukherjee, P.; Desai, P.; Avery, M. *Curr. Comput. Aided Drug Des.* **2010**, *6*, 1.
24. Carrat, F.; Bani-Sadr, F.; Pol, S.; Rosenthal, E.; Lunel-Fabiani, F.; Benzekri, A.; Morand, P.; Goujard, C.; Pialoux, G.; Piroth, L.; Salmon-Ceron, D.; Degott, C.; Cacoub, P.; Perronne, C. *J. Am. Med. Assoc.* **2004**, *292*, 2839.
25. Sijwali, P. S.; Kato, K.; Seydel, K. B.; Gut, J.; Lehman, J.; Klemba, M.; Goldberg, D. E.; Miller, L. H.; Rosenthal, P. J. *Proc. Natl. Acad. Sci. U.S.A.* **2004**, *101*, 8721.
26. Friesner, R. A.; Banks, J. L.; Murphy, R. B.; Halgren, T. A.; Klicic, J. J.; Daniel, T.; Repasky, M. P.; Knoll, E. H.; Shelley, M.; Perry, J. K. *J. Med. Chem.* **2004**, *47*, 1739.
27. Friesner, R. A.; Murphy, R. B.; Repasky, M. P.; Frye, L. L.; Greenwood, J. R.; Halgren, T. A.; Sanschagrin, P. C.; Mainz, D. T. *J. Med. Chem.* **2006**, *49*, 6177.
28. Jacobson, M. P.; Pincus, D. L.; Rapp, C. S.; Day, T. J. F.; Honig, B.; Shaw, D. E.; Friesner, R. A. *Proteins* **2004**, *55*, 351.
29. Jacobson, M. P.; Friesner, R. A.; Xiang, Z.; Honig, B. *J. Mol. Biol.* **2002**, *320*, 597.
30. Young, T.; Abel, R.; Kim, B.; Berne, B. J.; Friesner, R. A. *Proc. Natl. Acad. Sci. U.S.A.* **2007**, *104*, 808.
31. Abel, R.; Young, T.; Farid, R.; Berne, B. J.; Friesner, R. A. *J. Am. Chem. Soc.* **2008**, *130*, 2817.
32. Beuming, T.; Farid, R.; Sherman, W. *Protein Sci.* **2009**, *18*, 1609.
33. Robinson, D. D.; Sherman, W.; Farid, R. *ChemMedChem* **2010**, *5*, 618.
34. Higgs, C.; Beuming, T.; Sherman, W. *ACS Med. Chem. Lett.* **2010**, *1*, 160.
35. Pearlstein, R. A.; Hu, Q. Y.; Zhou, J.; Yowe, D.; Levell, J.; Dale, B.; Kaushik, V. K.; Daniels, D.; Hanrahan, S.; Sherman, W. *Proteins* **2010**, *78*, 2571.
36. Abel, R.; Salam, N. K.; Shelley, J.; Farid, R.; Friesner, R. A.; Sherman, W. *ChemMedChem* **2011**, *6*, 1049.
37. Shah, F.; Gut, J.; Legac, J.; Shivakumar, D.; Sherman, W.; Rosenthal, P. J.; Avery, M. A. *J. Chem. Inf. Model.* **2012**, *52*, 696.
38. Pellicciari, R.; Camaioni, E.; Gilbert, A. M.; Macchiarulo, A.; Bikker, J. A.; Shah, F.; Bard, J.; Costantino, G.; Gioiello, A.; Robertson, G. M. *Med. Chem. Commun.* **2011**, *2*, 559.
39. Turk, D.; Guncar, G.; Podobnik, M.; Turk, B. *Biol. Chem.* **1998**, *379*, 137.
40. Kerr, I. D.; Lee, J. H.; Farady, C. J.; Marion, R.; Rickert, M.; Sajid, M.; Pandey, K. C.; Caffrey, C. R.; Legac, J.; Hansell, E. *J. Biol. Chem.* **2009**, *284*, 25697.